Bridging the time gap: $Cu/ZnO/Al_2O_3$ methanol synthesis catalyst studied under industrial relevant conditions and time scales

Thomas Lunkenbein*, Frank Girgsdies, Timur Kandemir, Nygil Thomas, Malte Behrens, Robert Schlögl and Elias Frei*

Abstract

Long-term stability of catalysts is an important factor in chemical industry. This factor is often underestimated in academic testing protocols which may lead to a time-gap in the field of catalytic research. Here, we report on the deactivation behavior of an industrially relevant $Cu/ZnO/Al_2O_3$ catalyst for methanol synthesis over a period of 148 days time-on-stream, investigated by a combination of quasi *in-situ* and *ex-situ* analysis techniques. The results show that ZnO is the most dynamic species in the catalyst, whereas only slight changes can be observed in the Cu nanoparticles. Thus, the deactivation of this catalyst is driven by the changes in the ZnO moieties. Our findings indicate that methanol synthesis is an interface mediated process between Cu and ZnO.

Methanol, one of the most important industrial chemical, is produced from syngas (CO, CO_2, H_2) over ternary $Cu/ZnO/Al_2O_3$ catalyst at high pressure (50-80 bar) and elevated temperature (240-280 °C). Due to its high energy density (15.8 MJ/l), methanol is considered as a prospective key-compound for chemical energy and hydrogen storage.[1] However, its applicability as renewable fuel is still limited by the low efficiency cost intensive synthesis process. Improving and understanding this catalytic process is of great interest, but remains rather complex. Since the advent of more and more new sophisticated analysis tools the amount of generated knowledge in the field of “methanol synthesis” increased enormously. The majority of the produced data can be grouped into the following three different strategies: The first one generates mechanistic insights into the working catalysts with a pronounced theoretical support, often on model systems.[2] The second one deals with the empirical development of new and more efficient methanol catalysts.[3] The third group focuses on an increase of the catalytic stability of the industrial relevant catalysts.[4] To date, more than 95 % of the current academic research is based on the first two approaches. Although the working mechanisms of industrial methanol catalyst have been investigated extensively its actual active phase is still under debate and candidates range from pure Cu surfaces[5] over an active $Cu^{\delta+}$-O-Zn[6] interface and/or a synergy[7] between Cu-ZnO to an active CuZn surface alloy.[8] This catalytic odyssey may be caused by a diversity of different materials and synthesis/testing protocols that were applied, which often do not mirror industrially relevant conditions. The diversity of results further underlines the difficulty in investigating this complex catalyst material and show the importance of confining the applied industrial process parameters in the academic world.

The lifetime of an industrial applied catalyst for methanol synthesis is an important factor. As opposed to industrial protocols, standard academic test protocols reveal experiments of only a few hours time-on-stream (TOS) or the accelerated aging approach.[9] This suggests the presence of a time gap between industrially relevant and academic testing conditions. Thus, conclusions considering the long-term performance may be based on extrapolated data and/or are speculative. However, the development of a research concept interrogating the long-term stability requires the knowledge of the mechanism of deactivation. Here, we report on a study of the catalytic activity of an industrially relevant $Cu/ZnO/Al_2O_3$ catalyst over a period of 148 days TOS under relevant conditions [60 bar, 230 °C, syngas (8 CO_2 / 6 CO/ 59 H_2 / 27 inert)].

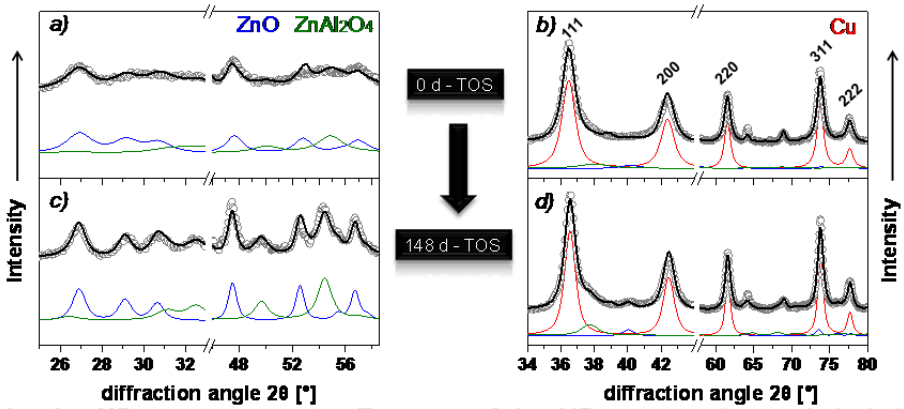

Figure 1. Quasi *in-situ* ND measurements. Excerpts of the ND patterns (grey circles) (a, c) after the first contact to the reaction feed (0 days) and (b, d) after 148 days TOS. The total fit curve (black), and the relevant phases Cu (red), ZnO (blue) and Zn,Al-spinel (green) are shown. The complete ND pattern is shown in the SI (Figure SI1).

Several grams of the industrial catalyst were retrieved from the catalysts bed after 0, 15, 30, 50, 102 and 148 days TOS. All batches were recovered and transferred without exposure to ambient air. Subsequently, the samples were analysed by a series of independent integral and differential methods ranging from quasi *in-situ* neutron diffraction (ND) over *ex-situ* techniques such as high resolution transmission electron microscopy (HRTEM), to surface sensitive measurements like specific surface area (BET-SA), N_2O reactive frontal chromatography (RFC) and H_2 transient adsorption (TA), which address all important components in this ternary catalyst systems.

ND is a suitable technique to characterize heterogeneous catalysts *in-situ* under working conditions and study their structural transformation.[10] The ND data provides important integral information like phase compositions and domain sizes of the catalyst material after different TOS. The parameters were extracted by full-pattern analysis with the Rietveld method using *TOPAS 5*[11] over a wide 2θ range. Figure 1 illustrates the ND pattern excerpts of Zn-containing phases and Cu, obtained after 0 days (Figure 1a, c) and 148 days (Figure 1b, d) TOS, respectively. The 0 days TOS sample was measured after reaching steady conditions under the respective pressure and temperature. For all measurements, the theoretical fit (black curve) agrees reasonably well with the experiment (grey circles) and shows only minor deviations. ND full patterns of Figure 1 and of all batches are provided in the supporting information.

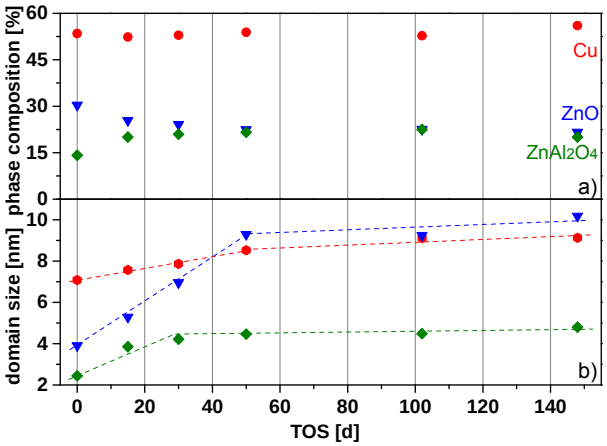

Figure 2. Quantitative analysis of the ND data. a) Phase composition of Cu, ZnO and Zn,Al-spinel of the catalysts over TOS. The data were obtained by Rietveld refinement of the ND patterns. b) Volume weighted mean domain sizes (L_{vol}-IB) of the corresponding phases, calculated from the width of the reflections. Red circles denote Cu nanoparticles, blue triangles correspond to ZnO and green diamonds represent Zn,Al-spinel.

Only reflections that correspond to metallic Cu (red curve), ZnO (blue curve) and $ZnAl_2O_4$ (green curve, Zn,Al-spinel) are observed. For the 0 days TOS, the weak reflections correspond to nanocrystalline ZnO and Zn,Al-spinel, respectively (Figure 1a). Metallic Cu^0 is the most dominant phase which can be assigned to the most pronounced reflections (Figure 1b). As opposed to the ND pattern of the 0 days TOS batch, the ND pattern of the catalyst removed after 148 days TOS (Figure 1c, d) consists of sharper reflections (see evolution of domain sizes, Figure 2). However, only minute changes in the sharpness of the ND reflections corresponding to Cu^0 can be found (Figure 1d). As highlighted in Figure 1c, the situation is different for the Zn-containing phases (ZnO and the Zn,Al-spinel). After the long-time experiment both oxide phases are significantly more crystalline compared to the initial sample. It should be noted that the fit model used, interprets the sample contribution to the ND peak broadening exclusively in terms of the size effect. While defects like strain or stacking faults certainly also contribute to some degree,[10a] a reasonable deconvolution of these factors is precluded by the complexity of the multi-phase pattern.

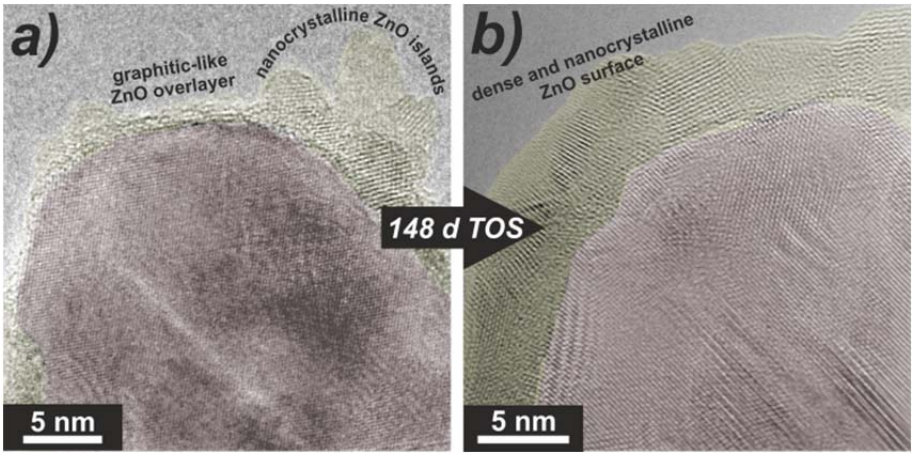

Figure 3. ZnO crystallization on Cu nanoparticles after TOS. TEM images of 0 days TOS (a) and 148 days TOS (b). ZnO moieties are colored yellow. Cu nanoparticles are highlighted in red. Original and further images are given in the SI.

As revealed by the quantitative evaluation of the ND patterns (Figure 2) the Cu content within the crystalline phases of the industrially relevant catalyst does not change significantly and remains almost constant at 50% for all TOS (Figure 2a). A more severe change is displayed in the content of ZnO and Zn,Al-spinel (Figure 2a). In the first 50 days TOS the catalyst is modified by an enrichment of the crystalline Zn,Al-spinel phase (14 to 21%), whereas in the same time frame the crystalline content of the ZnO phase is significantly reduced (30 to 23%). This trend indicates that initially amorphous Al-oxide species crystallize under reaction conditions into Zn,Al-spinel at the expanse of crystalline ZnO.

Figure 2b shows the domain sizes of Cu nanoparticles, ZnO and Zn,Al- spinel. The coherently scattering domain sizes of the Cu nanoparticles slightly increase (7.1±0.2 to 9.1±0.3 nm) during the prevailing time of the catalytic reaction (Figure 2b). The increase of the Cu crystallite size is in agreement with the observed slight sharpening of the reflections (Figure 1) and can be attributed to a weak sintering of the metal component. For the nanocrystalline Zn,Al-spinel a more pronounced increase in the domain sizes from 2.4±0.5 to 4.2±0.6 nm is found for the first 30 days TOS which remains constant for longer TOS. The ZnO nanoparticles exhibit the strongest modifications in the domain sizes in the first 50 days TOS. The coherently scattering domain is enlarged by 138% from 3.9±0.7 to 9.3±1.3 nm. Thus, the observed alterations in the ND pattern can be assigned to two competing processes that seem to be detrimental for the long-term stability of Cu based industrially relevant catalysts: (i) the formation and crystallization of Zn, Al-spinel and (ii) the sintering of the ZnO nanocrystals. To which extent one process influences or support the other process remains unclear,

but it seems likely that the crystallization of the Zn,Al-spinel occurs after the changes of the metastable ZnO phase into a phase stable under normal reaction conditions. The catalyst consists of 12 wt.% of Al^{3+}. Behrens et al.[3a] have shown that upon reductive activation, parts of the Al^{3+} (3-4 wt.%) will form a solid solution with the ZnO moieties which leads to structural and electronic promotion of the intrinsic catalytic performance. In addition, ZnO:Al also possess a higher sinter resistance compared to pure ZnO.[12] The excess Al^{3+} likely remains as ND amorphous γ-Al_2O_3, which is a defective spinel structure and can react with ZnO to dispersed Zn,Al-spinel (Figure 1) during methanol synthesis. After 30 days TOS the γ-Al_2O_3 is consumed and the absence of direct Zn,Al-spinel contacts may prevent further sintering. In the time period from 30 to 50 days TOS sintering and growth of the remaining ZnO nanoparticles continues. These two phenomena indicate that in an early TOS state the dissolved Al^{3+} in ZnO is also consumed and forms the spinel phase, which diminishes the sinter resistivity of ZnO. After 50 days TOS also the sintering of larger ZnO nanoparticles rapid flattens.

The mobility of the ZnO phase in the investigated industrial relevant Cu/ZnO/Al_2O_3 catalyst can be visualized by a comparative HRTEM study of batches retreived from the catalyst bed after 0 days TOS (Figure 3a) and 148 days TOS (Figure 3b). The overview TEM image in Figure S3a shows a porous microstructure of the catalyst after 0 days TOS with well separated particles. We recently, reported on the occurence of a graphitic-like ZnO_{1-x} overgrowth on top of the nanostructured Cu nanoparticles formed after reductive activation.[13] Here, the HRTEM images (Figure 3a, b) demonstrate a partial conversion of this metastable ZnO_{1-x} overgrowth into separated nano-islands on top of the Cu nanoparticles after contact to syngas at high pressures. In contrary, the overview image of the sample 148 days TOS (Figure S3e) shows a densely packed microstructure indicating the agglomeration of the catalyst. HRTEM images (Figure 3a, b) further reveal a dense poly-crystalline ZnO layer on top of defective Cu nanoparticles. No graphitic-like ZnO_{1-x} overgrowth was observed. In addition, all TEM images in Figure 3 and S3 suggest that the Cu nanoparticles are supporting the ZnO moieties.

The observed reflections in the detailed ND analysis arise from the stable wurtzite ZnO nanocrystals. The TEM images revealed severe changes in the local surface composition of the catalyst due to the transformation of the Zn containing phases which are initially kinetically stabilized, e.g. the ZnO_{1-x} overlayer and ZnO:Al phase. The reaction conditions (T, p) and the chemical potential of the gas feed induce the changes of the catalyst. In our case the sintering of the ZnO nanoparticles, the densification of the ZnO on the Cu surfaces and the Zn,Al-spinel formation are irreversible processes under the self-regulated chemical potential (see catalytic activity in Figure 4b). For instance, the metastable ZnO crystallites are converted into stable wurtzite ZnO and Zn,Al-spinel phases which represent the global minimum on the energy hyper-space under these conditions.

To study the consequences of the altered surface quantitatively in more detail, a sequence of different sorption experiments was conducted (Figure 4a). From nitrogen sorption experiments the specific BET-SA of the catalysts after different TOS were calculated and plotted in Figure 4a (red circles). The BET-SA decreases in the first 50 days TOS from 68 to 44 m^2/g and remains almost constant for longer TOS (44 to 39 m^2/g). N_2O-RFC measurements allow the quantification of the Cu surface area and redox active sites on ZnO, which are interpreted as oxygen vacancies in ZnO_{1-x} or Zn sites of a surface alloy[30] and are presented in Figure 4a (blue triangles).

The N_2O-SA shows a strong decrease from 19 to 14.5 m^2/g within the first 50 days TOS followed by a slight reduction of the N_2O-SA until 148 days TOS from 14.5 to 11 m^2/g. Due to measuring both Cu-SA and oxygen vacancies, a detailed interpretation of the N_2O-SA data can only be obtained if the pure Cu-SA is considered. The Cu-SA was measured applying the H_2-TA technique[14] (Figure 4a, black squares). The difference in N_2O-SA and Cu-SA can be interpreted as a measurement for the amount of partially reduced ZnO_x sites that likely play a synergistic role in methanol synthesis over Cu-based catalysts. The Cu-SA stays almost constant (~10 m^2/g) in the first 50 days TOS indicating that

the loss of the N_2O-SA can mostly be assigned to a reduction of the oxygen vacancies within the ZnO_{1-x} moieties. The behavior of the sorption experiments parallels the sintering course of the ZnO domains which also stopped after 50 days TOS.

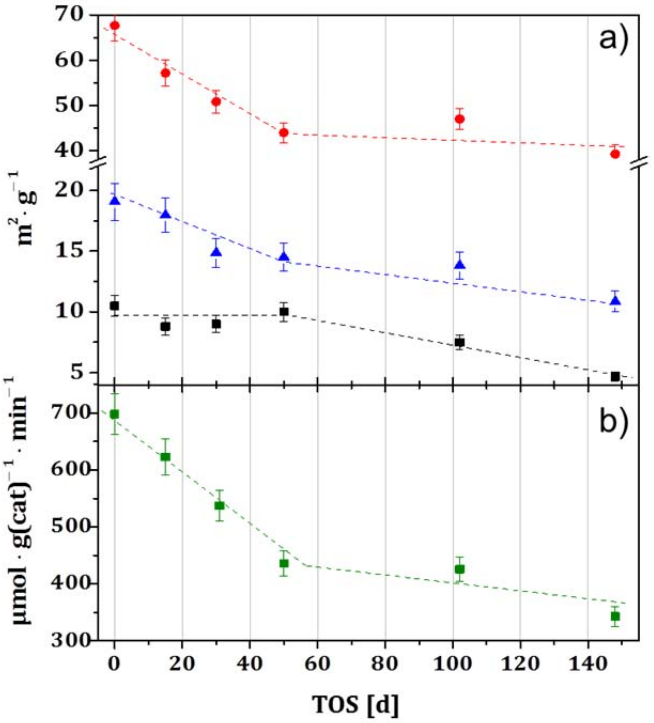

Figure 4. Surface characteristics and activity data of the catalyst for different TOS. a) Surface sensitive sorption measurements. Red circles denote the specific surface of the system as derived from the BET method. The blue triangles indicate N_2O-RFC measurements resulting in Cu surface area plus redox active sites on ZnO. Black squares represent the H_2-TA data that shows the actual Cu surface area. B) Activity data of the catalyst. All data are plotted against the TOS. The dashed lines are guides to the eye.

As soon as the ZnO domains are structurally stabilized, the Cu-SA starts to decrease from 10 to 5 m^2/g. According to Figure 2b, S3f and S3g, a dense and nanocrystalline layer of ZnO covers the Cu particles and limits the diffusion of N_2O and H_2 to the Cu surfaces.

In addition, the crystallization of the Zn-containing phases causes changes in the Cu/ZnO interface. These changes may induce a dynamic mesoscopic process (agglomeration) and can explain the slight decrease of the N_2O-SA and BET-SA from 50 to 148 days TOS.

The influence of the above mentioned structural and surface modifications on the catalytic activity in methanol synthesis is displayed in Figure 4b. Similar to the crystallization and sintering of the ZnO nanoparticles (Figure 1) as well as to the sorption experiments (Figure 4a) the rate of methanol production strongly decreases for the first 50 days TOS. However, for further TOS only a minor change can be observed. Thus, the catalytic activity can be directly correlated to the decrease of the surface properties. The intrinsic high activity accompanied with a metastable polymorph of ZnO underlines the relevance of high-energy structures generating the active phases in catalysis under reaction conditions.[15] Subsequent, energetically driven alteration of the ZnO moieties, including the induction of crystallization and sintering of ZnO causes a decrease in the catalytic activity, which can be also attributed to the loss of oxygen vacancies as shown by the N_2O measurements (Figure 3b). As opposed to shorter TOS where rapid sintering of ZnO and (Zn,Al) spinel is dominating the deactivation, after 50 days TOS “slow” sinter processes in the Zn containing phases and Cu nanoparticles (Figure 2b) are observed. This “slow” sinter processes flatten the H_2-TA curve (and N_2O-RFC, Figure 4a)

indicating that the loss in surface area is now not due to the covering of the Cu particles and the loss of interphase, but by the increased particle sizes. In addition, the results suggest that the minute changes of the Cu moieties (as main compound of the catalyst) have little impact on the performance of the catalyst within the first 50 days TOS, when the decisive deactivation occurs. The accessible Cu-SA remains almost stable for this time span, but the activity decreases enormously.

In conclusion, our findings lead to two new insights into industrially relevant $Cu/ZnO/Al_2O_3$ catalysts for methanol synthesis:

i) The early deactivation mechanism is dominated by the partial restructuring of the ZnO moieties associated with the re-crystallization of the whole ZnO phase. This influences the stability of the interface between ZnO and Cu. Furthermore, the finding highlights the role of ZnO being a co-catalyst rather than a ”support”, which prevents the Cu nanoparticles from sintering. It is therefore insufficient to describe industrially relevant methanol catalysts only with a Cu surface model. In addition, the copper surface area obtained by N_2O-RFC measurements are often interpreted as “Cu-SA”, although they also quantify additional redox active sites on reduced ZnO_{1-x}.[16] A possible scenario, in which the important role of Cu can be highlighted, is an interface mediated catalytic process between Cu-ZnO or $Cu^{\delta+}$-O-ZnO, which was already discussed in the literature as a candidate for the active phase.[6] The crystallization of ZnO moieties leads to a loss of this interface and to deactivation. This process explains the trends observed in the catalytic and surface sensitive data. Thus, the deactivation data excludes a surface alloy or unpromoted Cu as candidates for an active site. The $Cu/Cu^{\delta+}$-ZnO synergy (quantified by the difference of N_2O-SA and Cu-SA) is also strongly affected by the catalysts dynamics, but is still present at 148 days TOS (N_2O-SA > Cu-SA).

ii) The results of this longtime deactivation study demonstrate the importance of investigating the catalyst performance for industrial relevant TOS, which gives rise to a “time gap” in conventional academic studies. Besides, the “materials gap” underestimates the role of ZnO as the most mobile compound in the system. Finally, the control of the dynamic nature of ZnO under the working conditions and its promotion by Al^{3+} seems to be the key parameter for stabilizing the catalyst and its activity over a long TOS range.

Entry for the Table of Contents (Please choose one layout)

Layout 1:

TOC

ZnO the key for stability: As opposed to industry, long-term stability tests of catalysts are often underestimated in academia. We investigated the deactivation of industrially relevant Cu/ZnO/Al_2O_3 catalyst for methanol synthesis over a period of 148 days time-on-stream with a combination of quasi *in-situ* and *ex-situ* analysis techniques. Our findings indicate that controlling the polymorphism of ZnO is the

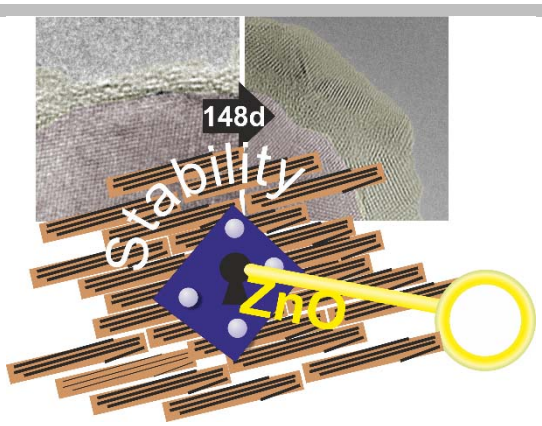

Thomas Lunkenbein, Timur Kandemir, Frank Girgsdies, Nygil Thomas, Malte Behrens, Robert Schlögl and Elias Frei**

ZnO dynamics: The deactivation mechanism of an industrially relevant Cu/ZnO/Al_2O_3 methanol synthesis catalyst

[1] a) F. Asinger, *Methanol - Chemie- und Energierohstoff: die Mobilisation der Kohle ; mit 175 Tabellen*, Akademie-Verlag, **1987**; b) A. G. George A. Olah, G. K. Surya Prakash *WILEY-VCH* **2011**; c) R. Schlögl, *Angewandte Chemie International Edition* **2015**, *54*, 4436-4439.

[2] a) L. C. Grabow, M. Mavrikakis, *ACS Catalysis* **2011**, *1*, 365-384; b) M. Behrens, F. Studt, I. Kasatkin, S. Kühl, M. Hävecker, F. Abild-Pedersen, S. Zander, F. Girgsdies, P. Kurr, B.-L. Kniep, M. Tovar, R. W. Fischer, J. K. Nørskov, R. Schlögl, *Science* **2012**, *336*, 893-897; c) F. Studt, M. Behrens, E. L. Kunkes, N. Thomas, S. Zander, A. Tarasov, J. Schumann, E. Frei, J. B. Varley, F. Abild-Pedersen, J. K. Nørskov, R. Schlögl, *ChemCatChem* **2015**, *7*, 1105-1111; d) Y. Yang, C. A. Mims, D. H. Mei, C. H. F. Peden, C. T. Campbell, *Journal of Catalysis* **2013**, *298*, 10-17.

[3] a) M. Behrens, S. Zander, P. Kurr, N. Jacobsen, J. Senker, G. Koch, T. Ressler, R. W. Fischer, R. Schlögl, *Journal of the American Chemical Society* **2013**, *135*, 6061-6068; b) J. Schumann, T. Lunkenbein, A. Tarasov, N. Thomas, R. Schlögl, M. Behrens, *ChemCatChem* **2014**, *6*, 2889-2897; c) E. Frei, A. Schaadt, T. Ludwig, H. Hillebrecht, I. Krossing, *ChemCatChem* **2014**, *6*, 1721-1730.

[4] a) M. B. Fichtl, D. Schlereth, N. Jacobsen, I. Kasatkin, J. Schumann, M. Behrens, R. Schlögl, O. Hinrichsen, *Applied Catalysis A: General* **2015**, *502*, 262-270; b) G. Prieto, J. Zečević, H. Friedrich, K. P. de Jong, P. E. de Jongh, *Nat Mater* **2013**, *12*, 34-39; c) S. Natesakhawat, P. R. Ohodnicki, B. H. Howard, J. W. Lekse, J. P. Baltrus, C. Matranga, *Topics in Catalysis* **2013**, *56*, 1752-1763; d) M. Twigg, M. Spencer, *Topics in Catalysis* **2003**, *22*, 191-203; eC. H. Bartholomew, *Applied Catalysis A: General* **2001**, *212*, 17-60; fH. H. Kung, *Catalysis Today* **1992**, *11*, 443-453.

[5] a) J. Yoshihara, C. T. Campbell, *Journal of Catalysis* **1996**, *161*, 776-782; b) M. Kurtz, N. Bauer, H. Wilmer, O. Hinrichsen, M. Muhler, *Chemical Engineering & Technology* **2004**, *27*, 1146-1150.
[6] K. Klier, *Adv. Catalysis* **1982**, *31*.
[7] a) J. Xiao, T. Frauenheim, *The Journal of Physical Chemistry Letters* **2012**, *3*, 2638-2642; bJ. Wang, S. Funk, U. Burghaus, *Catal Lett* **2005**, *103*, 219-223.
[8] a) Y. Choi, K. Futagami, T. Fujitani, J. Nakamura, *Applied Catalysis A: General* **2001**, *208*, 163-167; bM. S. Spencer, *Topics in Catalysis* **1999**, *8*, 259-266.
[9] J. Agrell, M. Boutonnet, I. Melián-Cabrera, J. L. G. Fierro, *Applied Catalysis A: General* **2003**, *253*, 201-211.
[10] a) T. Kandemir, F. Girgsdies, T. C. Hansen, K.-D. Liss, I. Kasatkin, E. L. Kunkes, G. Wowsnick, N. Jacobsen, R. Schlögl, M. Behrens, *Angewandte Chemie* **2013**, *125*, 5271-5276; b) T. Kandemir, D. Wallacher, T. Hansen, K.-D. Liss, R. Naumann d'Alnoncourt, R. Schlögl, M. Behrens, *Nuclear Instruments and Methods in Physics Research Section A: Accelerators, Spectrometers, Detectors and Associated Equipment* **2012**, *673*, 51-55.
[11] B. A. G. Topas 5, **2015**.
[12] J. Schumann, M. Eichelbaum, T. Lunkenbein, N. Thomas, M. C. Álvarez Galván, R. Schlögl, M. Behrens, *ACS Catalysis* **2015**, *5*, 3260-3270.
[13] T. Lunkenbein, J. Schumann, M. Behrens, R. Schlögl, M. G. Willinger, *Angewandte Chemie International Edition* **2015**, *54*, 4544-4548.
[14] a) S. Kuld, C. Conradsen, P. G. Moses, I. Chorkendorff, J. Sehested, *Angewandte Chemie* **2014**, *126*, 6051-6055; b) O. Hinrichsen, T. Genger, M. Muhler, in *Studies in Surface Science and Catalysis, Vol. Volume 130* (Eds.: F. V. M. S. M. Avelino Corma, G. F. José Luis), Elsevier, **2000**, pp. 3825-3830.
[15] R. Schlögl, *Angewandte Chemie International Edition* **2015**, *54*, 3465-3520.
[16] a) M. B. Fichtl, J. Schumann, I. Kasatkin, N. Jacobsen, M. Behrens, R. Schlögl, M. Muhler, O. Hinrichsen, *Angewandte Chemie International Edition* **2014**, *53*, 7043-7047; b) K. C. Waugh, *Catalysis Today* **1992**, *15*, 51-75; cG. C. Chinchen, K. C. Waugh, D. A. Whan, *Applied Catalysis* **1986**, *25*, 101-107.